Supramolecular Phosphorescent Trinuclear Copper(I) Pyrazolate Complexes for Vapochromic Chemosen....

Article *in* Indonesian Journal of Chemistry · July 2017

DOI: 10.22146/ijc.22553

3 authors:

Hendrik Oktendy Lintang
Ma Chung University
104 PUBLICATIONS **257** CITATIONS
SEE PROFILE

Nur Fatiha Ghazalli
Universiti Malaysia Terengganu
3 PUBLICATIONS **3** CITATIONS
SEE PROFILE

Leny Yuliati
Ma Chung University
108 PUBLICATIONS **567** CITATIONS
SEE PROFILE

Supramolecular Phosphorescent Trinuclear Copper(I) Pyrazolate Complexes for Vapochromic Chemosensors of Ethanol

Hendrik Oktendy Lintang[1,2,3,*], Nur Fatiha Ghazalli[4,5], and Leny Yuliati[1,2,3]

[1]*Ma Chung Research Center for Photosynthetic Pigments, Universitas Ma Chung, Malang 65151, East Java, Indonesia*

[2]*Department of Chemistry, Faculty of Science and Technology, Universitas Ma Chung, Malang 65151, East Java, Indonesia*

[3]*Centre for Sustainable Nanomaterials, Ibnu Sina Institute for Scientific and Industrial Research, Universiti Teknologi Malaysia, 81310 UTM Johor Bahru, Johor, Malaysia*

[4]*Department of Chemistry, Faculty of Science, Universiti Teknologi Malaysia, 81310 UTM Johor Bahru, Johor, Malaysia*

[5]*Pusat Pengajian Sains Asas, Universiti Malaysia Terengganu, 21030 Kuala Terengganu, Terengganu, Malaysia*

Received February 27, 2017; Accepted July 11, 2017

ABSTRACT

*We highlight that by using supramolecular single crystals of phosphorescent trinuclear copper(I) pyrazolate complexes with different molecular structures (**2**$_{A-E}$), vapochromic chemosensors were successfully designed for sensing ethanol with high sensing capability. These complexes **2**$_{A-E}$ were synthesized from non-side chain, 3,5-dimethyl, 3,5-bis(trifluoromethyl), 3,5-diphenyl and 4-(3,5-dimethoxybenzyl)-3,5-dimethyl pyrazole ligands (**1**$_{A-E}$) in 83, 97, 99, 88 and 85% yields, respectively. All complexes showed emission bands centered at 553, 584, 570 and 616 nm upon an excitation at 280 nm for complexes **2**$_{A-C,E}$, respectively and 642 nm upon an excitation at 321 nm for complex **2**$_D$ with lifetime in microseconds, indicating a large Stoke shift for phosphorescent compounds. These emission spectra were in good agreement with their colors from green to red upon exposure to a UV lamp with an excitation at 254 nm in dark room. Upon exposure to ethanol in 5 min, quenching, photoinduced energy transfer and shifting of emission intensities were observed for chemosensors **2**$_{A-C}$, **2**$_D$ and **2**$_E$, respectively. Interestingly, chemosensor **2**$_E$ only showed completely and autonomously recovery of its original emission intensity. Such novel finding in sensing capability might be caused by a weak intermolecular hydrogen bonding interaction of ethanol to oxygen atoms at dimethoxybenzyl side-chains of the pyrazole ring.*

Keywords: *ethanol; phosphorescent properties; trinuclear copper(I) pyrazolate complexes; vapochromic chemosensor*

ABSTRAK

*Kami menyoroti bahwa dengan menggunakan kristal tunggal supramolekul dari kompleks tembaga(I) pirazolat tiganuklir pendarfosfor dengan perbedaan struktur molekul, vapokromik kemosensor telah dengan berhasil dirancang untuk mendeteksi etanol dengan kemampuan deteksi tinggi. Kompleks **2**$_{A-E}$ ini masing-masing telah disintesis dari ligan pirazol (**1**$_{A-E}$) tidak berantai samping, 3,5-dimetil, 3,5-bis(trifluorometil), 3,5-difenil dan 4-(3,5-dimetoksibensil)-3,5-dimetil dengan hasil 83, 97, 99, 88 dan 85%. Semua kompleks masing-masing menunjukkan pita emisi berpusat pada 553, 584, 570 and 616 nm dengan eksitasi pada 280 nm untuk kompleks **2**$_{A-C,E}$, dan 642 nm dengan eksitasi pada 321 nm untuk kompleks **2**$_D$ dengan waktu paruh dalam mikrodetik, menunjukkan pergeseran Stoke yang besar untuk senyawa-senyawa pendarfosfor. Spektrum-spektrum emisi ini bersesuaian dengan baik dengan warna-warnanya dari hijau ke merah dengan menghadapkan ke lampu UV pada eksitasi 254 nm di dalam ruangan gelap. Dengan menghadapkan terhadap etanol selama 5 menit, penurunan, fotoinduksi perpindahan energi dan pergeseran dari intensitas emisi masing-masing telah diamati untuk kemosensor **2**$_{A-C}$, **2**$_D$ dan **2**$_E$. Menariknya, kemosensor **2**$_E$ hanya menunjukkan pemulihan intensitas emisi aslinya secara menyeluruh dan mandiri. Temuan baru seperti ini dengan kemampuan mendeteksi mungkin disebabkan oleh interaksi ikatan lemah hidrogen antara molekul dengan atom oksigen pada dimetoksibensil berantai samping dari cincin pirazol.*

Kata Kunci: *etanol; sifat pendarfosfor; kompleks tembaga(I) pirazolat tiganuklir; vapokromik kemosensor*

* Corresponding author. Tel : +62-341-550171
Email address : hendrik.lintang@machung.ac.id

DOI: 10.22146/ijc.22553

INTRODUCTION

Volatile organic compounds (VOCs) are generally well-known as one of pollutants from industrial processes due to their effects on environment and human health [1]. Particularly, alcohol derivatives such ethanol have been found as VOCs which can effect on human immunity for long-term by inducing inhibition and stimulation into the bodies [2]. These VOCs have encouraged many researchers to develop chemical sensors (chemosensors) optically with high sensing capabilities in sensitivity, selectivity and reusability as well as low-cost precursors [3-4]. By using organic chromophores as a chemosensor, the detection of the vapors with organic chromophores (vapochromics) as chemosensors have been studied to evaluate the changes in luminescence (color, emission intensity and lifetime) [5], absorption (transmittance) [6], thermal resistivity [7], refractive index [8], swelling [9], mass [9], permittivity [10] and etc.

Optical chemosensors based on the changes in luminescent properties have been widely developed due to their sensitivities over other methods [11]. Since phosphorescent compounds are indicated by its longer luminescent lifetime from the metal-metal interactions than the fluorescence, many complexes from d^6, d^8 and d^{10} metal ions with extended π-system or coordination donors have been synthesized as phosphorescent metal complexes. The resulting metal complexes have revealed color changes from vapor-triggered luminescence owing to metal-solvent, metal-metal, π-π, hydrogen bonding and host-guest interactions [12]. In this case, supramolecular phosphorescent metal complexes with their self-assembling properties have been extensively explored as chemosensors due to possibility of changes in tunability and rigidity [13-14]. For example, Nagel and co-workers in 1988 [15] synthesized palladium (Pd) and platinum (Pt) double-complex or mixed salt for the detection of vapors. This type of complex was fabricated into fibre optics for the detection of VOCs by Lancaster 1995 [16]. In 1998, Maan and co-workers have successfully synthesized Pt-Pt double-complex salt for vapochromic sensors of organic vapors with color, absorption and emission changes [17]. In Group 11, gold complexes or bimetallic gold-silver complexes with various types of ligands have been also reported as chemosensors [18]. Although copper complexes can be synthesized using less expensive precursors and showed a strong luminescent intensity and longer lifetime, they have received less attention as chemosensors so far [19]. Therefore, it would be interesting to develop new phosphorescent chemosensors using copper complexes with high sensing capability for detection of VOCs such ethanol. Previously, we have reported that phosphorescent trinuclear copper(I) pyrazolate complexes from 3,5-dimethyl and 4-(3,5-dimethoxybenzyl)-3,5-dimethyl pyrazole ligands were successfully synthesized and then used for chemosensors of ethanol [20]. In particular, we have found that trinuclear copper(I) 4-(3,5-dimethoxybenzyl)-3,5-dimethyl pyrazolate complex only showed a positive response to ethanol by shifting the emission band from 604 to 554 nm where the original intensity can be recovered without external stimuli. Therefore, in this continuous study, we are particularly focused on the sensing capability of vapochromic copper complexes from a series of pyrazole ligands with different molecular structures at their side-chains. It is expected that upon exposure to ethanol, the chemosensors will show the importance of molecular structure in supramolecular self-assembly of single crystal phosphorescent complexes with different rigidity, electronegativity and metal-metal distance for their sensing capabilities. Indeed, we found that, trinuclear copper(I) 4-(3,5-dimethoxybenzyl)-3,5-dimethyl pyrazolate complex (chemosensor $\mathbf{2_E}$) showed the best sensing capabilities from the changes in emission spectra (616 to 555 nm) and images (orange to green). These results suggest that such sensing capability for chemosensor $\mathbf{2_E}$ might be caused by a weak intermolecular hydrogen bonding interaction between hydroxy group (OH) of ethanol with electronegative O atoms at the methoxy group in the benzyl of the pyrazole ring.

EXPERIMENTAL SECTION

Materials

All the reagents and chemicals were used in analytical grade that were purchased from Sigma-Aldrich, while all the solvents were used in anhydrous grade. Triethylamine (Et_3N) was distilled under vacuum and nitrogen (N_2) condition where the collecting fraction was stored in dry potassium hydroxide (KOH).

Instrumentation

Fourier transform infrared spectroscopy (FT-IR) was used on Thermo Scientific model a Nicolet iS50 using potassium bromide (KBr) to make a pellet. Mass spectra were recorded by electrospray ionization (ESI) source for ionization using JEOL model a JMS–T100LP (AccuTOF LC–plus). Sample was firstly prepared in dichloromethane (DCM) with addition of methanol (MeOH) or acetone for direct injection method with quantity of 10 μL/min and needle voltage of 2000 V. Structure analysis was performed on Bruker AXS Diffract plus release 2000 model of X-ray diffractometer (XRD) in the range of 2θ at 2–40° with a scan rate of

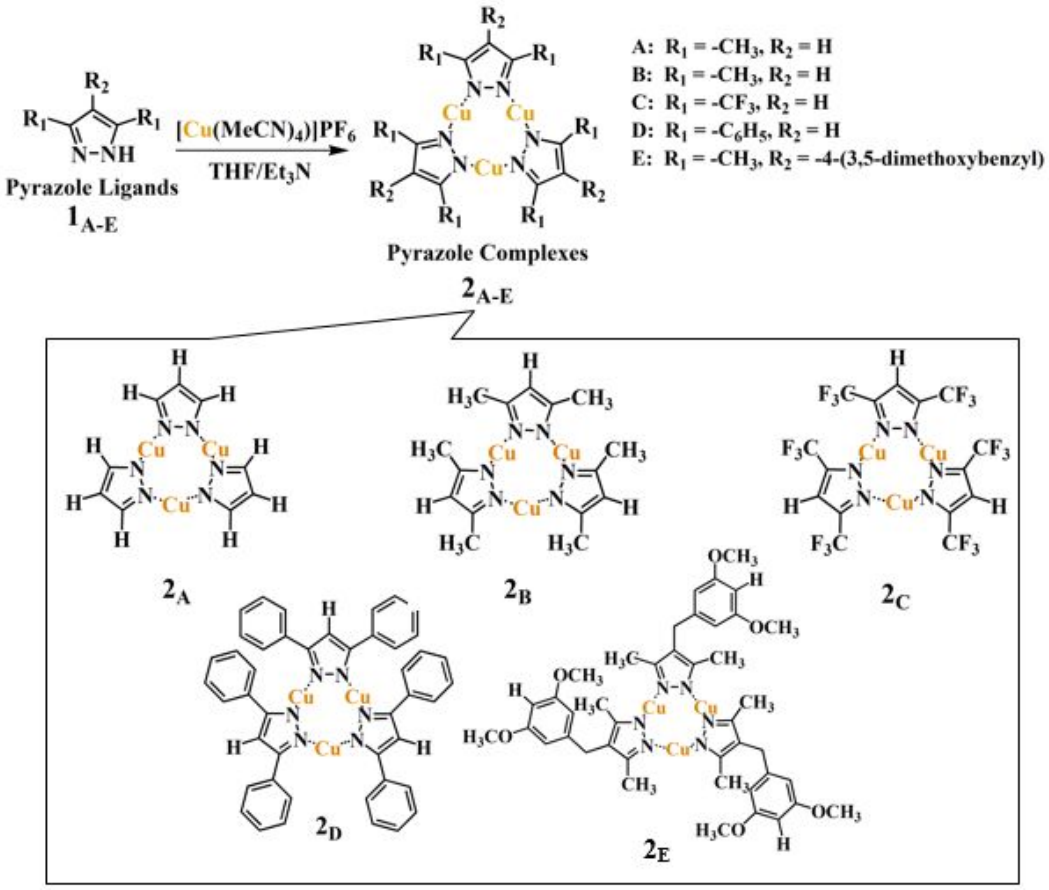

Fig 1. Syntheses and molecular structures of complexes 2_{A-E} from pyrazole ligands 1_{A-E} with different alkyl side-chains

0.02° s^{-1}. Absorption spectra were measured using Shimadzu Diffuse Reflectance (DR) Ultraviolet-Visible (UV-Vis) spectrophotometer (UV-2600) for solids samples (barium sulfate; Ba_2SO_4 was used as the reference). JASCO spectrofluorophotometer with model of FP–8500 was used to evaluate luminescence properties. Photographs were taken by using Panasonic Lumix Camera (DMC–FZ38) with a macro zoom under a UV lamp (Vilber Lourmat, 8 watt) at daylight or in the dark room. The PTI QuantaMaster 400 Horiba with near infrared (NIR) PMT detector model 914 under liquid nitrogen cooling system was used as steady state photoluminescent spectrometer for determination of emission and excitation maxima in the lifetime measurement with a Xenon lamp (75 W) in microsecond time scale.

Procedure

Synthesis of trinuclear pyrazolate copper(I) complexes

Trinuclear copper(I) pyrazolate complexes were synthesized by a Schlenk technique using five types of pyrazole ligands from non-side chain, 3,5-dimethyl, 3,5-bis(trifluoromethyl), 3,5-diphenyl and 4-(3,5-dimethoxybenzyl)-3,5-dimethyl in the presence of copper(I) ions from tetrakis(acetonitrile)copper(I)hexa fluorophosphate ($[Cu(MeCN)_4]PF_6$) according to previous report by Kishimura et al. [21] (Fig. 1). Typically, at room temperature, the mixture of pyrazole ligand and $[Cu(MeCN)_4]PF_6$ in tetrahydrofuran (THF) was stirrer for 5 min and followed by adding the distilled Et_3N under an inert condition. After overnight reaction, THF was removed from the reaction mixture under reduce pressure and the remaining residues were dried off to isolate the desired complexes. For purification, *in–situ* recrystallization was carried out by dissolving the desired complexes in DCM (15 mL) under an inert condition. This solution was added dropwisely into dry MeOH at room temperature for complexes $\mathbf{2_{A-E}}$. In this condition, the resulting crystals were filtered by *in-situ* filtration and followed by washing few time with dry MeOH. The resulting residues were dried off to give solid powder or sticky of the $\mathbf{2_{A-E}}$. The collected complexes were evaporated and then dried under reduce of vacuum pressure to give $\mathbf{2_{A-E}}$ in 83, 97, 99,

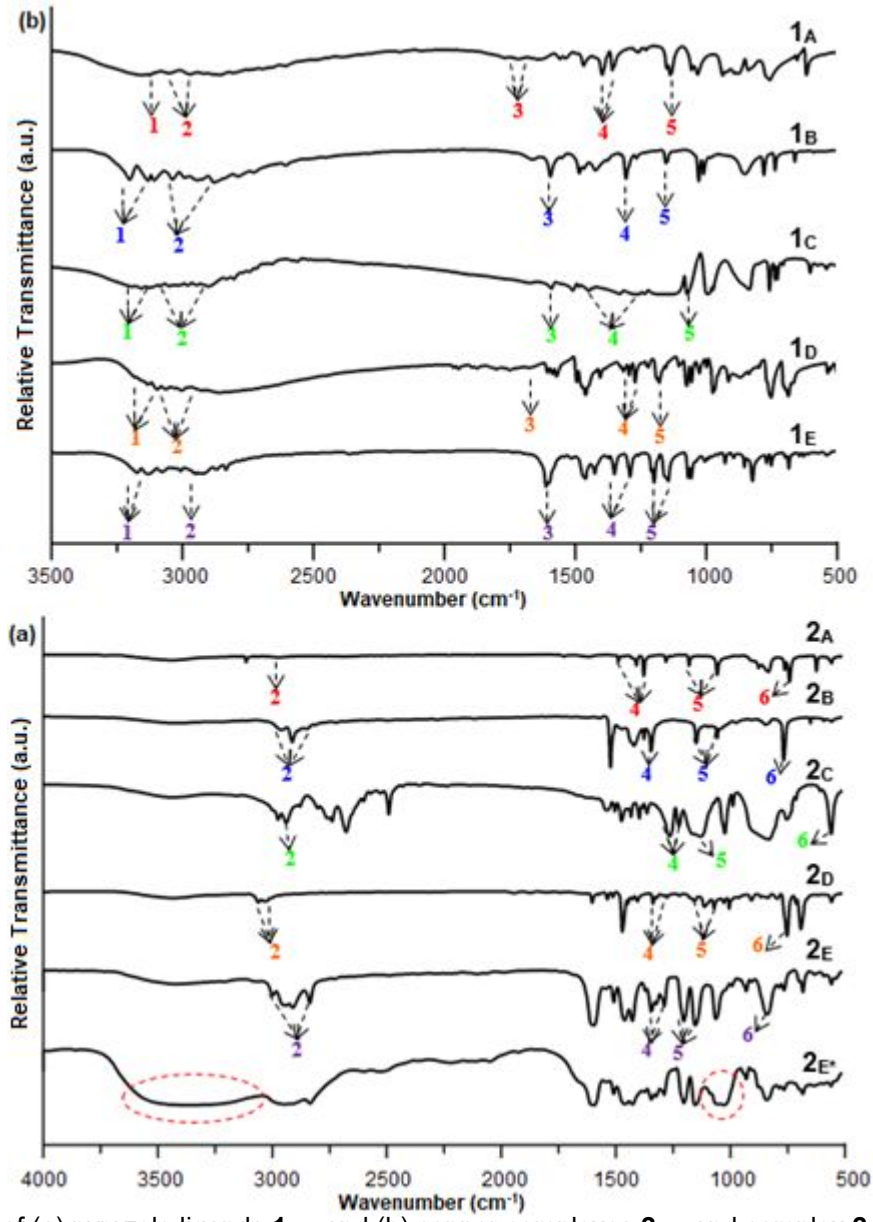

Fig 2. FT-IR spectra of (a) pyrazole ligands $\mathbf{1}_{A\text{-}E}$ and (b) copper complexes $\mathbf{2}_{A\text{-}E}$ and complex $\mathbf{2}_{E}$ (labeled as $\mathbf{2}_{E}$*) after exposure to ethanol vapor for 5 min

88 and 85% yields, respectively.

Sensing capability

For evaluation of sensing capability, complexes $\mathbf{2}_{A\text{-}E}$ in 22 mg as chemosensors were directly exposed to 8.7 ppm (200 μL) of ethanol vapor from 0 to 5 min. The study was carried out by arranging cell holder for spectrofluorophotometer containing of the chemosensors into the sealed beaker for exposure in 1-5 min. After completion of the exposure time, the sensing capabilities were directly evaluated using spectrofluorophotometer.

RESULT AND DISCUSSION

Structure Elucidation of Chemosensors

In order to confirm the synthesis of copper(I) complexes, FT-IR and mass spectroscopy measurements were carried out to observe characteristic vibration bands of functional groups and molecular weight for the ligands $\mathbf{1}_{A\text{-}E}$ and desired complexes $\mathbf{2}_{A\text{-}E}$. Fig. 2 shows FT-IR spectra of the ligands $\mathbf{1}_{A\text{-}E}$ and their copper complexes $\mathbf{2}_{A\text{-}E}$ with characteristic vibration bands at wavenumber of 3500-500 cm^{-1}. For the ligands as shown in Fig. 2a, the

Table 1. The FT-IR data for pyazole ligands $\mathbf{1}_{A-E}$ and copper complexes $\mathbf{2}_{A-E}$

Samples	Functional Groups (cm^{-1})					
	N–H stretch	C–H stretch	N–H bend	C–N stretch	N–N stretch	Cu–N
$\mathbf{1}_A$	3124 (m, 1)	2971-2807 (m, 2)	1722-1643 (w, 3)	1397-1358 (s, 4)	1150-1137 (s, 5)	–
$\mathbf{1}_B$	3201-3109 (m, 1)	3038-2878 (m, 2)	1595 (s, 3)	1306 (s, 4)	1154-1148 (m, 6)	–
$\mathbf{1}_C$	3157-3058 (w, 1)	3049-2901 (w, 2)	1677 (m, 3)	1329-1235 (w, 4)	1073 (w, 5)	–
$\mathbf{1}_D$	3133-3096 (w, 1)	3063-2856 (m, 2)	1750 (m, 3)	1316-1271 (m, 4)	1180 (m, 5)	–
$\mathbf{1}_E$	3173-3133 (m, 1)	2948 (m, 2)	1611 (s, 3)	1350-1290 (s, 4)	1199-1145 (m, 5)	–
$\mathbf{2}_A$	–	2985 (w, 2)	–	1504-1378 (m, 4)	1181-1058 (w, 5)	742 (w, 6)
$\mathbf{2}_B$	–	2959-2848 (m, 2)	–	1346 (m, 4)	1148-1058 (m, 5)	767 (w, 6)
$\mathbf{2}_C$	–	2975 (m, 2)	–	1266-1226 (m, 4)	1131 (m, 5)	560 (w, 6)
$\mathbf{2}_D$	–	3061-3031 (w, 2)	–	1338-1278 (w, 4)	1155-1071 (w, 5)	714 (w, 6)
$\mathbf{2}_E$	–	2999-2835 (w, 2)	–	1371-1289 (m, 4)	1289-1155 (m, 5)	832 (w, 6)

Note: In the bracket for the functional groups, s, m and w are referred to strong, medium and weak vibrations while the number are referred to the vibration peaks at FT-IR spectra

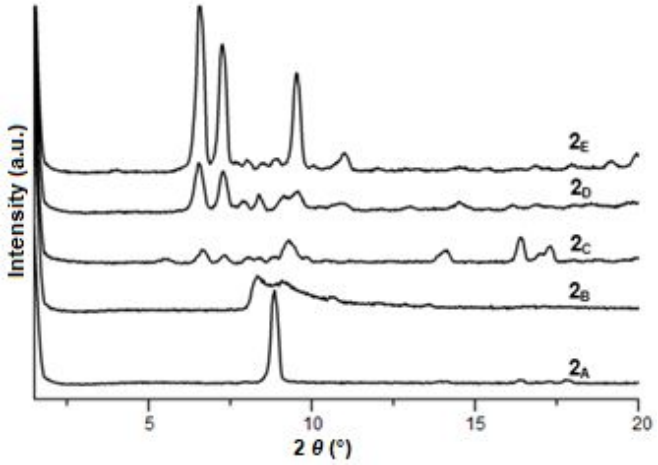

Fig 3. X-ray patterns of copper complexes $\mathbf{2}_{A-E}$

vibration bands at 3201-3058 cm^{-1} (***1***) and 1750-1595 cm^{-1} (**3**) (Table 1) were assigned to N–H stretching and bending from 1° or 2° amine groups. These N–H vibration bands of pyrazole ligands did not observe in that of the pyrazolate complexes due to the formation of N–Cu–N with the vibration band at 560-832 cm^{-1} (**6**) while the complexes still preserved the C–H, C–N and N–N stretchings of the ligands with vibration bands at 2971-2817 cm^{-1} (**2**), 1397-1358 cm^{-1} (**4**) and 1150-1137 cm^{-1} (**5**) (Table 1), respectively. Based on the mass spectra, the monoisotopic patterns for $\mathbf{2}_A$ and $\mathbf{2}_B$ with molecular formula of $C_9H_9Cu_3N_6$ and $C_{15}H_{21}Cu_3N_6$ showed intense peaks at 391.8793 Da ($\mathbf{2}_A$) and 475.9119 Da ($\mathbf{2}_B$) for observed molecular weight of $[M+H]^+$, which were closed to 392.8760 and 476.9700 Da of the calculated molecular weight. For $\mathbf{2}_C$ and $\mathbf{2}_D$ with molecular formula of $C_{15}H_3Cu_3F_{18}N_6$ and $C_{45}H_{33}Cu_3N_6$ ($[M+Na]^+$ at 822.7902 and 871.0544 Da for $\mathbf{2}_C$ and $\mathbf{2}_D$), the peaks of molecular weight were observed at 822.3446 Da ($\mathbf{2}_C$) and 871.5956 Da ($\mathbf{2}_D$) for $[M+Na]^+$. The monoisotopic patterns for both complexes displayed almost similar to the prediction ones. Moreover, the observed molecular weight for $\mathbf{2}_E$ was obtained at 927.6032 Da, which was similar to the isotopic pattern with the calculated molecular formula of $C_{42}H_{51}Cu_3N_6O_6$ ($[M+H]^+$ at 927.1827 Da). Therefore, we have successfully synthesized complexes $\mathbf{2}_{A-E}$ in high yields in the range of 83 to 99%. Of interest, Fig. 3 shows the X-ray patterns for all copper(I) complexes with characteristic diffraction peaks, suggesting the formation of semi-crystalline structure.

Optical Properties of Chemosensors

Molecular geometry and optical properties of luminescent d^{10} complexes have been found to show the characteristic of chemosensors in particular applications [22]. For example, trinuclear metal pyrazolate complexes with different from their substituents and metals on ligands have been reported to show interesting bright and tunable luminescence properties [23]. Moreover, by controlling the elongation of the assembly or shortening the distance of metal-metal interactions, the self-assembled structures can be tuned using intermolecular metallophilic interaction of

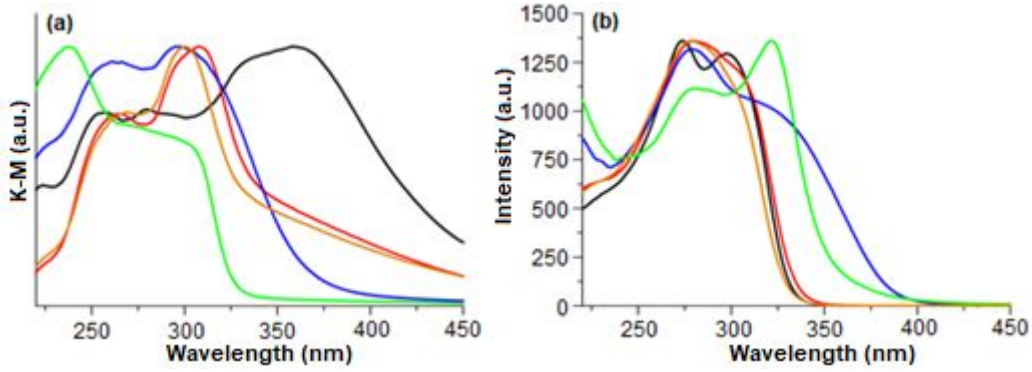

Fig 4. (a) Absorption and (b) excitation spectra of copper complexes $\mathbf{2_A}$ (λ_{em} = 553 nm, black solid line), $\mathbf{2_B}$ (λ_{em} = 584 nm, red solid line), $\mathbf{2_C}$ (λ_{em} = 570 nm, blue solid line), $\mathbf{2_D}$ (λ_{em} = 644 nm, green solid line) and $\mathbf{2_E}$ (λ_{em} = 616 nm, orange solid line)

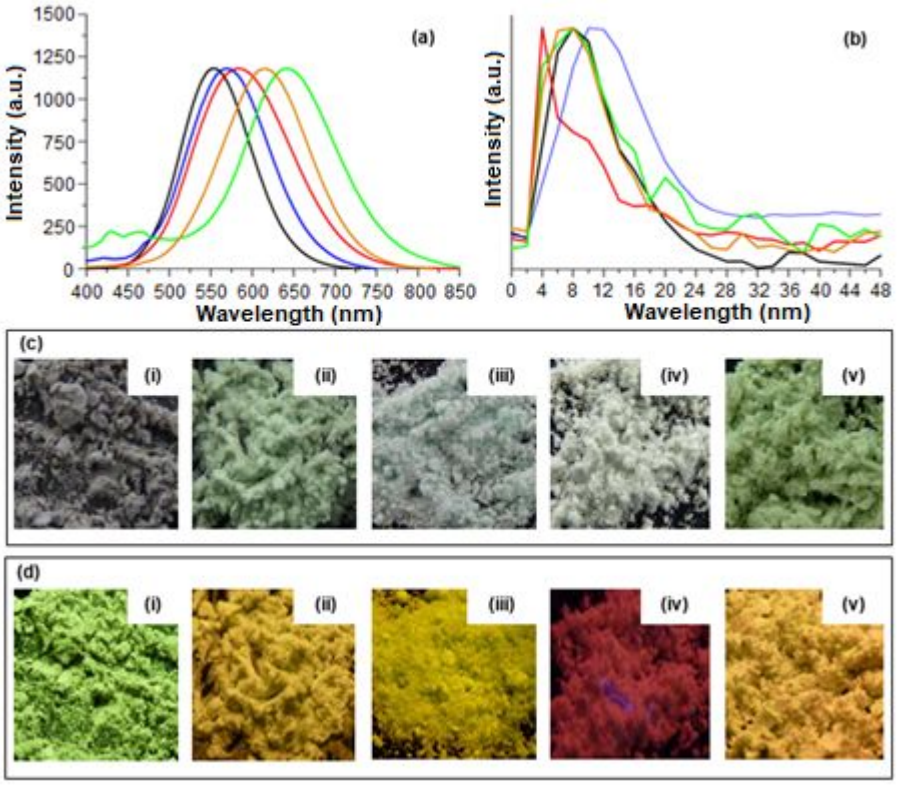

Fig 5. (a) Normalized emission spectra and (b) phosphorescence decay profile for copper complexes $\mathbf{2_A}$ (λ_{ext} = 274 nm, λ_{em} = 553 nm, black solid line), $\mathbf{2_B}$ (λ_{ext} = 280 nm, λ_{em} = 584 nm, red solid line), $\mathbf{2_C}$ (λ_{ext} = 280 nm, λ_{em} = 570 nm, blue solid line), $\mathbf{2_D}$ (λ_{ext} = 322 nm, λ_{em} = 644 nm, green solid line) and $\mathbf{2_E}$ (λ_{ext} = 278 nm, λ_{em} = 616 nm, orange solid line) and (c) their photography images at daylight and (d) dark condition at room temperature upon exposure with a UV hand lamp at 254 nm of (i) copper complexes $\mathbf{2_A}$, (ii) $\mathbf{2_B}$, (iii) $\mathbf{2_C}$, (iv) $\mathbf{2_D}$ and (v) $\mathbf{2_E}$

the metal complexes [24]. Spectroscopically, the luminescence properties of complexes $\mathbf{2_{A-E}}$ were performed using DR UV-Vis spectrometer and photoluminescent spectrofluorometer [25]. The absorption spectra were measured to find the maximum energy for excitation of electrons from ground to excited state in the emission measurement. Fig. 4a shows DR UV-Vis spectra with the peak tops of 280-358, 307, 296, 304 and 300 nm for complexes $\mathbf{2_{A-E}}$, respectively. The range of absorption bands are originated by $\pi \rightarrow \pi^*$ transitions in the conjugated double bonds of the aromatic rings.

By using the peak top of absorption spectra as an excitation wavelength (λ_{ext}), the luminescent properties from the emission spectra were measured for each complex. Fig. 5a shows the emission spectra as well as

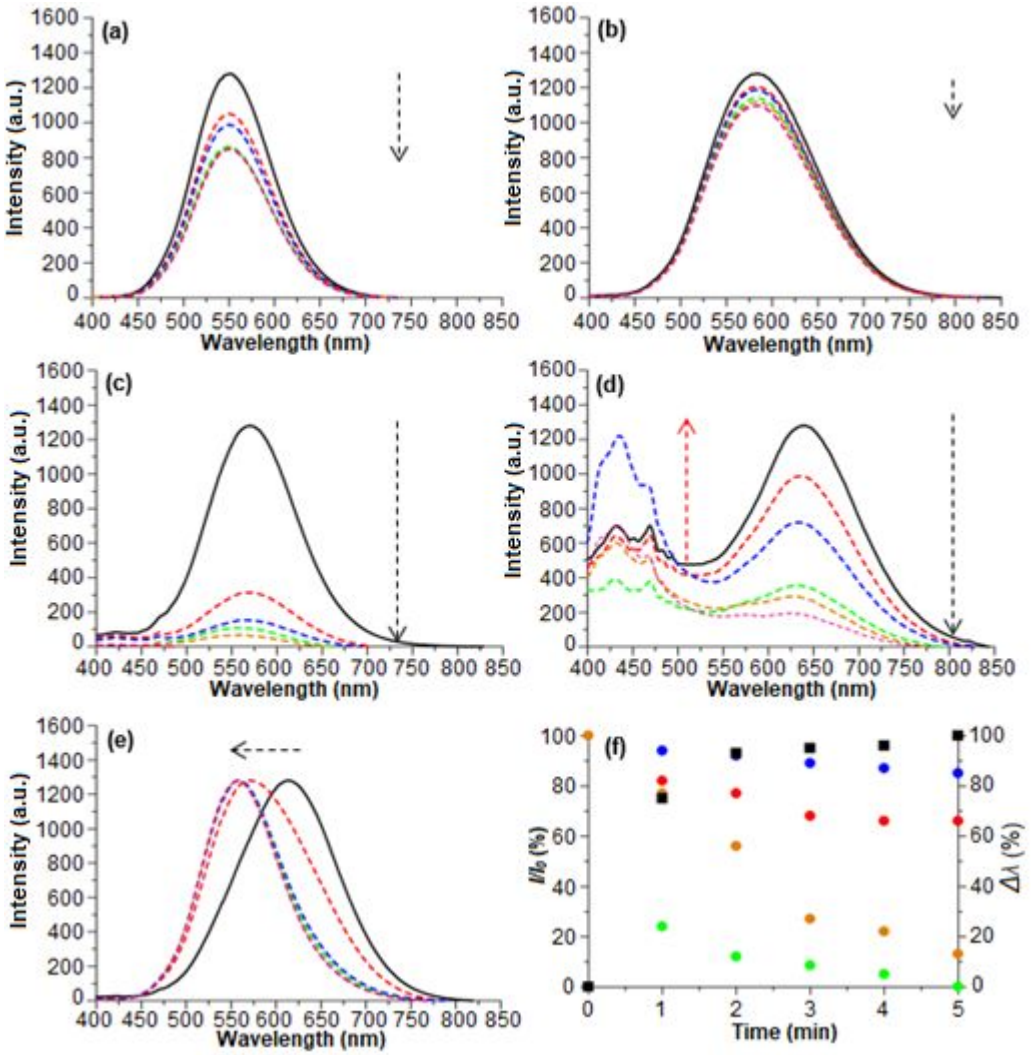

Fig 6. Emission spectral changes of (a) chemosensors $\mathbf{2_A}$ (λ_{ext} = 274 nm) (b) $\mathbf{2_B}$ (λ_{ext} = 280 nm) (c) $\mathbf{2_C}$ (λ_{ext} = 280 nm), (d) $\mathbf{2_D}$ (λ_{ext} = 322 nm) and (e) $\mathbf{2_E}$ (λ_{ext} = 278 nm) upon exposure to ethanol from 0 (black solid line), 1 (red dash line), 2 (blue dash line), 3 (green dash line), 4 (orange dash line) to 5 min (pink dash line) as well as (f) their changes in emission intensities for chemosensors $\mathbf{2_A}$ (553 nm, red dot), $\mathbf{2_B}$ (584 nm, blue dot), $\mathbf{2_C}$ (570 nm, green dot), $\mathbf{2_D}$ (644 nm, orange dot) and Stokes shift for chemosensor $\mathbf{2_E}$ (616 nm, black square)

their colors at daylight (Fig. 5c) and in the dark room under exposure to a UV hand lamp at 254 nm (Fig. 5d). The emission spectra showed a peak centered at 553, 584, 570, 644 and 616 nm for complexes $\mathbf{2_{A\text{-}E}}$ (Fig. 5a), which were in good agreement with their colors as green, orange, greenish, red and orange under exposure to a UV hand lamp at 254 nm in the dark room (Fig. 5d), respectively. Monitoring at these emission wavelengths (λ_{em}), it provided the excitation spectra for maximum absorption wavelengths with a peak centered at 274, 280, 280, 275-322 and 278 nm for complexes $\mathbf{2_{A\text{-}E}}$ (Fig. 4b), which were closed to the peak top of luminophores in the DR UV-Vis spectra (Fig. 4a). Such luminescent profile gave a large Stokes shift ($\Delta\lambda$) in 279, 304, 290, 322 and 338 nm, indicating the characteristics of phosphorescent compounds [21,23-34]. Moreover, the luminescent decay measurements in excitation and emission maxima as shown in Fig. 5b were evaluated to give phosphorescent lifetime (τ) = 7.44±0.7, 7.60±1.5, 7.37±0.4, 8.69±0.3 and 8.16±1.8 μs at room temperature for complexes $\mathbf{2_{A\text{-}E}}$, respectively. Hence, complexes $\mathbf{2_{A\text{-}E}}$ were successfully confirmed as phosphorescent compounds by metal-centered triplet excited states of the weak Cu(I)–Cu(I) metallophilic interaction [19,23-27]. Considering the advantages of copper(I) complexes in their phosphorescence properties, it can be developed as promising vapochromic chemosensors based on changes in optical properties upon exposure to VOCs [35].

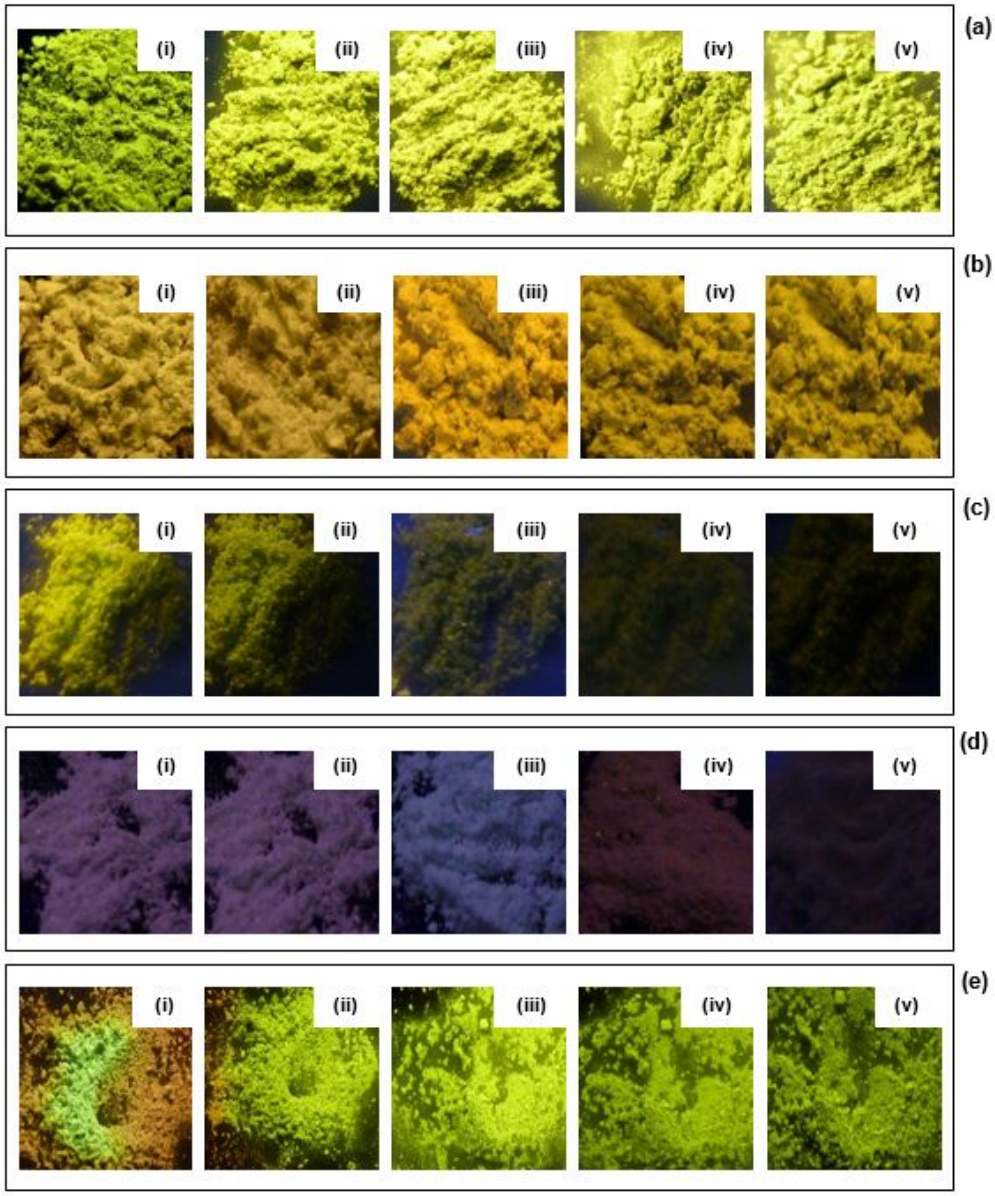

Fig 7. Photography images of (a) chemosensors $\mathbf{2_A}$ (b) $\mathbf{2_B}$ (c) $\mathbf{2_C}$ (d) $\mathbf{2_D}$ and (e) $\mathbf{2_E}$ upon exposure to ethanol for (i) 1, (ii) 2, (iii) 3, (iv) 4 and (v) 5 min. The photographs were taken at room temperature on exposure to a UV hand lamp at 254 nm in the dark room

Sensing Capability of Chemosensors

Sensing capabilities [35] were evaluated by monitoring the changes in emission intensities and colors for the specific exposure time. Fig. 6 shows emission spectral changes upon exposure to ethanol (8.7 ppm) from 0 to 5 min. Three phenomena were observed; quenching for chemosensors $\mathbf{2_{A\text{-}C}}$ (Fig. 6a-c), photoinduced energy transfer for chemosensor $\mathbf{2_D}$ (Fig. 6d) and shifting for chemosensor $\mathbf{2_E}$ (Fig. 6e). For the quenching phenomenon, upon excitation at 280 nm in 0 min, it displayed an emission band centered at 553 nm for $\mathbf{2_A}$, 584 nm for $\mathbf{2_B}$, and 570 nm for $\mathbf{2_C}$ (black solid line in Fig. 6a-c). Upon exposure for 1-5 min, chemosensor $\mathbf{2_A}$ showed decreasing in its intensity (Fig. 6a, dash line) up to 18, 23, 32, 33 and 34% respectively as shown in Fig. 6f (red dot). It clearly showed that the emission intensity was almost saturated in 3 min where the changes in color emission were appeared from high contrast (Fig. 5d(i)) to less intense of green-yellowish images (Fig. 7a(i-v)). When pyrazole ligand has 3,5-dimethyl (two of $–CH_3$) at the side-chain of the ring for chemosensor $\mathbf{2_B}$, the decreasing in emission intensity (Fig. 6b, dash line) were

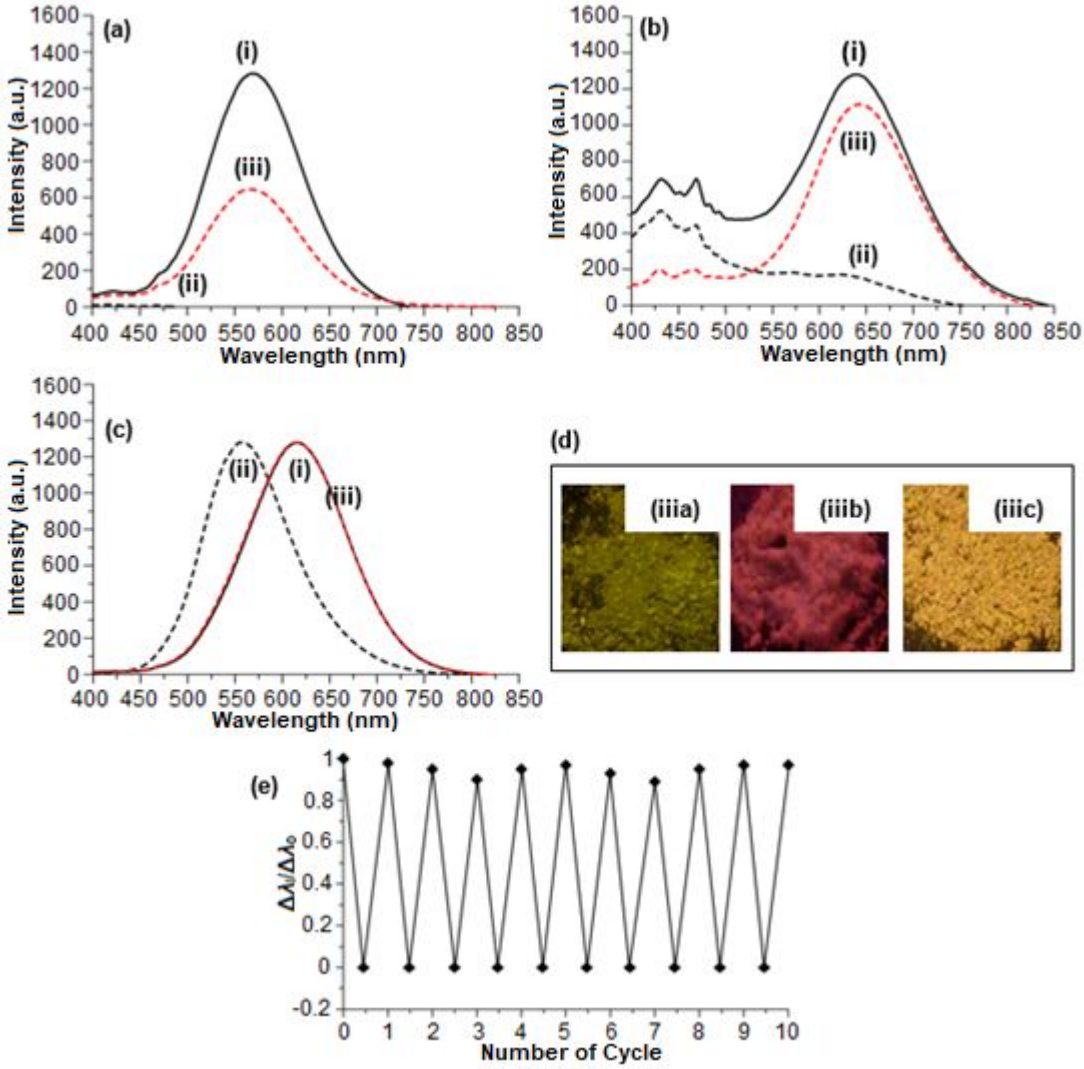

Fig 8. Emission spectral changes of (a) chemosensors $\mathbf{2_C}$ (λ_{ext} = 280 nm), (b) $\mathbf{2_D}$ (λ_{ext} = 322 nm) and (c) $\mathbf{2_E}$ (λ_{ext} = 278 nm) upon exposure to ethanol from (i) 0 (black solid line) to (ii) 5 min (black dash line) and (iii) their reversible changes (red dash line), (d) photography images on reusability test for (iiia) chemosensors $\mathbf{2_C}$, (iiib) $\mathbf{2_D}$ and (iiic) $\mathbf{2_E}$ at room temperature on exposure to a UV hand lamp at 254 nm in the dark room, and (e) reusability test of chemosensor $\mathbf{2_E}$ up to 10 cycles

only in 6% of quenching intensity after exposure for 1 min and in 15% after 5 min (Fig.6f, blue dot). It was finally saturated in 5 min (Fig. 6b, dash line), which were in good agreement with almost no color changes of their orange emissions (Figs. 5d(ii) and 7b). When we used bis(trifluoromethyl) (two of $–CF_3$) at *meso*-position of the pyrazole ring, the chemosensor $\mathbf{2_C}$ displayed significantly decline of its emission intensity (Fig. 6c, dash line) in 76% even for exposure with ethanol in 1 min and then achieved in 100% after 5 min (Fig. 6f, green dot). Such quenching of intensity in 100% indicates that the *chair-like* coordination geometry of Cu(I)-Cu(I) metallophilic interaction [4,19-27,35] was totally disrupted through the columnar assembly of the weak intermolecular interaction. In this case, Cu(I) ions in one pyrazole ring are unable to form metal-metal interaction with other Cu(I) ions of the ligand. Monitoring color emission in the dark room, it was in good agreement with their color changes from bright (Fig. 5d(iii)) to less intense of green emission in the first 2 min (Fig. 7c(i-ii)) and then became less emissive as a dark image in 3 to 5 min (Fig. 7c(iii-v)). Although chemosensor $\mathbf{2_C}$ gave 100% quenching, the original intensity can be only recovered up to 51% (Fig. 8a(iii)) with less emissive of green emission (Fig. 8d(iiia)) upon external stimuli such as heating and grinding. Therefore, these phenomena suggest that the molecular structure of chemosensors with a short alkyl side chain at the pyrazole ring of the

complexes gave significant effect on the sensing capability with quenching phenomena toward the ethanol vapors. Since molecular size of ethanol is not large enough to cut-off the metal-metal interaction among pyrazolate molecules, such changes in emission spectra [3-5,12-20] and colors [4,12,35] in quenching phenomenon might be caused by the formation of a weak intermolecular hydrogen bonding interaction [4,13,18-20,25-27,35] from OH of ethanol vapors with electronegative N and/or F atoms at the pyrazole ring so that the metal-metal interaction was totally disrupted and cannot form a bonding between the molecules. In the presence of bulky side chains from $–CH_3$, the sensing capability will be reduced due to the influence of accessibility of ethanol vapors from that bulky group to be diffused to the emission center.

Energy transfer is one of phenomena in sensing capability due to the formation of a new emission site while the former emission site is coincidentally changed to a non-emissive site [30,35]. Upon exposure to ethanol for 1 min (Fig. 6d, dash line), chemosensor $\mathbf{2_D}$ shows that its original emission centered at 644 nm was quenched in 23% (Fig. 6f, orange dot) while two new emission bands at 436 and 460 nm were appeared for possible formation of aggregation induced emission at the phenyl side-chains of the pyrazole ring [36]. When it was exposed above 1 min, the emission center was gradually quenched (Fig. 6d, dash line) up to 44, 73, 78 and 87% in 2-5 min (Fig. 6f, orange dot) which were well supported by their color changes from red (Fig. 5d(iv)) to less intense of red or light pink (Fig. 7d(i-ii), white (Fig. 7d(iii)) and dark red emission (Fig. 7d(iv-v)) in 2, 3 and 4-5 min. Considering ethanol vapors tend to interact as explained above, it probably provides changes in the molecular distance at the phenyl of the pyrazole ring and their metal-metal interactions so that such changes in emission spectra and colors suggest the occurrence of photoinduced energy transfer from metal-metal interactions to phenyl side-chains of the pyrazole ring. Similar to chemosensor $\mathbf{2_C}$, under external stimuli, the original intensity can be only recovered around 87% (Fig. 8b(iii)) with less emissive of red emission (Fig. 8d(iiib)).

Shifting of emission [20] center can be also used to evaluate sensing phenomena due to a weak interaction of analytes to either metal-metal interaction or electronegative atom at outside molecule to give shorter (red shift) or longer (blue shift) distance of metal-metal interaction. Upon exposure to ethanol, chemosensor $\mathbf{2_E}$ shows that its original emission centered at 616 nm was blue-shifted to 560, 558 and 557 nm (Fig. 6e) in 2-4 mins with $\Delta\lambda$ in 56, 58 and 59 nm (Fig. 6f, black square). Finally, the emission band was shifted to 555 nm with $\Delta\lambda$ in 61 nm and the color was changed from orange (Fig. 5d(v)) to green (Fig. 7e). Since chemosensor $\mathbf{2_E}$ has shorter metal-metal distance (616 nm) than chemosensors $\mathbf{2_{A\text{-}C}}$ (553, 584 and 570 nm) based on their emission centers (Fig. 6a-c), ethanol will probably difficult to be diffused to short distance of the metal-metal interaction. Hence, such changes in emission spectra and colors might be caused by interaction of OH of ethanol with electronegative O atoms of the methoxy groups at the benzyl ring via a weak intermolecular hydrogen bonding interaction to give increasing in the metal-metal distance. This week interaction gave perfectly and autonomously recovery of its emission intensity (Fig. 8c(iii)) and color (Fig. 8d(iiic)) in 15 min to the original phosphorescent properties.

Based on the evaluation of sensing capability, chemosensor $\mathbf{2_E}$ showed the best performance compared to others. Therefore, further experiment was carried out for reusability test, which is one of the important criteria for selecting sensor materials. As mentioned in previous paragraph, chemosensor $\mathbf{2_E}$ still gave perfectly and autonomously recovery of its original emission intensity in 15 min. In contrast to chemosensors $\mathbf{2_C}$ and $\mathbf{2_D}$, this performance for the reusability test of chemosensor $\mathbf{2_E}$ can be achieved even up to 10 cycles (Fig. 8e). Moreover, limit of detection (LOD) for chemosensor $\mathbf{2_E}$ was calculated using IUPAC definition as 3σ/slope [37] that gave 0.013 ppm. These results indicate that chemosensor $\mathbf{2_E}$ has high reusability and sensitivity the detection of ethanol vapors.

In order to confirm the interaction of chemosensor $\mathbf{2_E}$ toward the ethanol vapors after exposure for 5 min, FTIR analysis was carried out as shown in Fig. 2b (chemosensor $\mathbf{2_E}$ after exposure to vapor was labeled as $\mathbf{2_E}$* with particular vibration peaks at red circles). It was found that a new broad peak was clearly observed at 3383 cm^{-1} for vibration of O–H from hydrogen bonding while vibration peak for the C–H stretching at 2939 cm^{-1} was changed to a broad and less intense peak. Such a weak intermolecular hydrogen bonding interaction between OH of ethanol to $O–CH_3$ at dimethoxybenzyl side-chains of the pyrazole ring was confirmed by the change of sharp peak at 1064 cm^{-1} for the vibration O–C from the methoxy group at the side-chains (before exposure) to broad one peak at 1029 cm^{-1} with a shoulder at 1064 cm^{-1}. Hence, chemosensor $\mathbf{2_E}$ shows the best sensing capability upon exposure to ethanol vapors.

CONCLUSION

In conclusion, we have successfully synthesized 5 types of trinuclear copper(I) pyrazolate complexes ($\mathbf{2_{A\text{-}E}}$) from non-side chain, 3,5-dimethyl, 3,5-bis(trifluoromethyl), 3,5-diphenyl and 4-(3,5-dimethoxy

benzyl)-3,5-dimethyl pyrazole ligands ($\mathbf{1}_{\mathbf{A-E}}$) in 83, 97, 99, 88 and 85% yields. All complexes showed characteristic phosphorescent properties with emission bands centered at 553, 590, 570, 642 and 616 nm, large Stokes shifts and luminescent lifetime decays in the range of 7.37 to 8.69 μs, which were in good agreement with their colors from green, orange, greenish, red and orange, respectively. Upon exposure to ethanol, except chemosensor $\mathbf{2}_{\mathbf{B}}$, three sensing phenomena as a positive response were evaluated as quenching for chemosensors $\mathbf{2}_{\mathbf{A-C}}$ with color OFF, photoinduced energy transfer for chemosensor $\mathbf{2}_{\mathbf{D}}$ with color OFF, and blue-shifting for chemosensor $\mathbf{2}_{\mathbf{E}}$ with color change from orange to green. Based on the sensing capability with changes in spectra and images, chemosensor $\mathbf{2}_{\mathbf{E}}$ was found to be the best of sensors for the detection of ethanol vapors due to the presence of electronegative O atoms at the methoxy group in the benzyl of the pyrazole ring for the weak intermolecular hydrogen bonding interaction. By using molecular designs in the synthesis of metal complexes as phosphorescent chemosensors, high sensing capability can be achieved for the detection of VOCs in next future.

ACKNOWLEDGEMENT

The authors thank Universiti Malaysia Terengganu (UMT) and Ministry of Higher Education (MOHE), Malaysia for the financial support as well as Centre for Sustainable Nanomaterials, Ibnu Sina Institute for Scientific and Industrial Research (ISI-SIR), Universiti Teknologi Malaysia (UTM), Malaysia for characterization facilities. The authors also thank consultancy project with vote no. 1079 from RGS Corporation Sdn. Bhd. through Uni-Technologies Sdn. Bhd., Malaysia for the financial supports.

REFERENCES

[1] Elosua, C., Bariain, C., Matias, I.R., Rodriguez, A., Colacio, E., Salinas-Castillo, A., Segura-Carretero, A., and Fernandez-Gutiérrez, A., 2008, Pyridine vapors detection by an optical fibre sensor, *Sensors*, 8 (2), 847–859.

[2] Mikov, I., Mikov, A., Siriski, J., Mikov, M., and Milovanov, V., 2000, Effect of simultaneous exposure to benzene and ethanol on urinary phenol excretion in mice, *J. Occup. Health*, 42 (5), 258–259.

[3] Prodi, L., Bolletta, F., Montalti, M., and Zaccheroni, N., 2000, Luminescent chemosensors for transition metal ions, *Coord. Chem. Rev.*, 205 (1), 59–83.

[4] Zhang, X., Li, B., Chen, Z.H., and Chen, Z.N., 2012, Luminescence vapochromism in solid materials based on metal complexes for detection of volatile organic compounds (VOCs), *J. Mater. Chem.*, 22 (23), 11427–11441.

[5] Krytchankou, I.S., Koshevoy, I.O., Gurzhiy, V.V., Pomogaev, V.A., and Tunik, S.P., 2015, Luminescence solvato-and vapochromism of alkynyl-phosphine copper clusters, *Inorg. Chem.*, 54 (17), 8288–8297.

[6] Pu, S., Ma, L., Liu, G., Ding, H., and Chen, B., 2015, A multiple switching diarylethene with a phenyl-linked rhodamine B unit and its application as chemosensor for Cu^{2+}, *Dyes Pigm.*, 113, 70–77.

[7] Peng, H., Stich, M.I.J., Yu, J., Sun, L.N., Fischer, L.H., and Wolfbeis, O.S., 2010, Luminescent europium(III) nanoparticles for sensing and imaging of temperature in the physiological range, *Adv. Mater.*, 22, 716–719.

[8] Elosúa, C., Bariáin, C., Matías, I.R., Arregui, F.J., Luquin, A., and Laguna, M., 2006, Volatile alcoholic compounds fibre optic nanosensors, *Sens. Actuators, B*, 115, 444–449.

[9] Macagnano, A., Perri, V., Zampetti, E., Bearzotti, A., and De Cesare, F., 2016, Humidity effects on a novel eco-friendly chemosensor based on electrospun PANi/PHB nanofibres, *Sens. Actuators, B*, 232, 16–27.

[10] Endres, H.E., Hartinger, R., Schwaiger, M., Gmelch, G., and Roth, M., 1999, A capacitive CO_2 sensor system with suppression of the humidity interference, *Sens. Actuators, B*, 57 (1-3), 83–87.

[11] Xu, Z., Chen, X., Kim, H.N., and Yoon, J., 2010, Sensors for the optical detection of cyanide ion, *Chem. Soc. Rev.*, 39 (1), 127–137.

[12] Kobayashi, A., and Kato, M., 2014, Vapochromic platinum(II) complexes: Crystal engineering toward intelligent sensing devices, *Eur. J. Inorg. Chem.*, 2014 (27), 4469–4483.

[13] Bell, T.W., and Hext, N.M., 2004, Supramolecular optical chemosensors for organic analytes, *Chem. Soc. Rev.*, 33 (9), 589–598.

[14] Mancin, F., Rampazzo, E., Tecilla, P., and Tonellato, U., 2006, Self-assembled fluorescent chemosensors, *Chem. Eur. J.*, 12 (7), 1844–1854.

[15] Nagel, C.C., 1998, Preparation of vapochromic double complex salts, *Eur. Pat. Appl. EP*, 277003.

[16] Lancaster, G.D., Moore, G.A., Stone, M.L., and Reagen, W.K., 1995, Volatile organic compound sensing devices, *U.S. Patent 5*, 445795.

[17] Mann, K.R., Daws, C.A., Exstrom, C.L., Janzen, D.E., and Pomije, M., 1998, Vapochromic platinum-complexes and salts, *U.S. Patent 5*, 766952.

[18] Wenger, O.S., 2013, Vapochromism in organometallic and coordination complexes:

chemical sensors for volatile organic compounds, *Chem. Rev.*, 113 (5), 3686–3733.

[19] Enomoto, M., Kishimura, A., and Aida, T., 2001, Coordination metallacycles of an achiral dendron self-assemble via metal-metal interaction to form luminescent superhelical fibers, *J. Am. Chem. Soc.*, 123 (23), 5608–5609.

[20] Ghazalli, N.F., Yuliati, L., Endud, S., Shamsuddin, M., and Lintang, H.O., 2014, Vapochromic copper(I) pyrazolate complex materials for phosphorescent chemosensors of ethanol, *Adv. Mater. Res.*, 970, 44–47.

[21] Kishimura, A., Yamashita, T., and Aida, T., 2005, Phosphorescent organogels via "metallophilic" interactions for reversible RGB-color switching, *J. Am. Chem. Soc.*, 127 (1), 179–183.

[22] Hu, B., Gahungu, G., and Zhang, J., 2007, Optical properties of the phosphorescent trinuclear copper(I) complexes of pyrazolates: Insights from theory, *J. Phys. Chem. A*, 111 (23), 4965–4973.

[23] Dias, H.R., Polach, S.A., and Wang, Z., 2000, Coinage metal complexes of 3,5-bis (trifluoromethyl) pyrazolate ligand: synthesis and characterization of {[3,5-(CF3)2Pz] Cu}3 and {[3,5-(CF3)2Pz] Ag}3, *J. Fluorine Chem.*, 103 (2), 163–169.

[24] Kishimura, A., 2005, Novel luminescent materials based on the self–assembly via metal–metal interactions among group 11 metal ions, *Thesis*, University of Tokyo, GI1 – GI35 and III1-III27.

[25] Dias, H.R., Diyabalanage, H.V., Eldabaja, M.G., Elbjeirami, O., Rawashdeh-Omary, M.A., and Omary, M.A., 2005, Brightly phosphorescent trinuclear copper(I) complexes of pyrazolates: Substituent effects on the supramolecular structure and photophysics, *J. Am. Chem. Soc.*, 127 (20), 7489–7501.

[26] Dias, H.R., Diyabalanage, H.V., Rawashdeh-Omary, M.A., Franzman, M.A., and Omary, M.A., 2003, Bright phosphorescence of a trinuclear copper(I) complex: Luminescence thermochromism, solvatochromism, and "concentration luminochro mism", *J. Am. Chem. Soc.*, 125 (40), 12072–12073.

[27] Kishimura, A., Yamashita, T., Yamaguchi, K., and Aida, T., 2005, Rewritable phosphorescent paper by the control of competing kinetic and thermodynamic self-assembling events, *Nat. Mater.*, 4, 546–549.

[28] Lintang, H.O., Kinbara, K., Tanaka, K., Yamashita, T., and Aida, T., 2010, Self-repair of a one-dimensional molecular assembly in mesoporous silica by a nanoscopic template effect, *Angew. Chem. Int. Ed.*, 49 (25), 4241–4245.

[29] Lintang, H.O., Kinbara, K., Yamashita, T., and Aida, T., 2010, Heating effect of a one-dimensional molecular assembly on self-repairing capability in the nanoscopic channels of mesoporous silica, *Proceedings of International Conferences on Enabling Science and Nanotechnology (ESciNano)*, Article Number 5700970, ISBN: 978-1-4244-8853-7.

[30] Lintang, H.O., Kinbara, K., Tanaka, K., Yamashita, T., and Aida, T., 2012, Metal-ion permeation in congested nanochannels: The exposure effect of Ag^+ ions on the phosphorescent properties of a gold(I)–pyrazolate complex that is confined in the nanoscopic channels of mesoporous silica, *Chem. Asian J.*, 7 (9), 2068–2072.

[31] Lintang, H.O., Kinbara, K., and Aida, T., 2012, Thermally resistive phosphorescent molecular assembly in the channels of mesoporous silica nanocomposites, *Proceedings of International Conferences on Enabling Science and Nanotechnology (ESciNano)*, Article Number 6149684, ISBN: 978-1-4577-0799-5.

[32] Lintang, H.O., Yuliati, L., and Endud, S., 2014, Phosphorescent sensing and imaging of temperature using mesoporous silica/gold nanocomposites, *Mater. Res. Innovations*, 18, S6-444–S6-448.

[33] Jalani, M.A., Yuliati, L., Endud, S., and Lintang, H.O., 2014, Synthesis of mesoporous silica nanocomposites for preparation of gold nanoparticles, *Adv. Mater. Res.*, 925, 233–237.

[34] Jalani, M.A., Yuliati, L., Lintang, H.O., 2014, Thermal hydrogen reduction for synthesis of gold nanoparticles in the nanochannels of mesoporous silica composite, *Jurnal Teknologi*, 70 (1), 131–136.

[35] Zhao, Q., Li, F., and Huang, C., 2010, Phosphorescent chemosensors based on heavy-metal complexes, *Chem. Soc. Rev.*, 39 (8), 3007–3030.

[36] Sathish, V., Ramdass, A., Thanasekaran, P., Lu, K.L., and Rajagopal, S., 2015, Aggregation-induced phosphorescence enhancement (AIPE) based on transition metal complexes–an overview, *J. Photochem. Photobiol., C*, 23, 25–44.

[37] Analytical Methods Committee, 1987, Recommendations for the definition, estimation, and use of detection limit, *Analyst*, 112, 199–204.